One-year lunar calibration result of Hodoyoshi-1, Moon as an ideal target for small satellite radiometric calibration

Toru Kouyama, Ryosuke Nakamura
National Institute of Advanced Industrial Science and Technology
2-3-26, Aomi, Koto-ku, Tokyo, 135-0064, Japan; +81-29-29-861-2506
t.kouyama@aist.go.jp

Soushi Kato
Remote Sensing Technology Center of Japan
3-17-1 Toranomon, Minato-ku, Tokyo, 105-0001, Japan; +81-3-6435-6700
kato_soushi@restec.or.jp

Naoki Miyashita
Axelspace Corporation
3-3-3 Nihonbashi-Honcho, Chuo-ku, Tokyo, 103-0023, Japan; +81-3-4405-5085
miyashita@axelspace.com

ABSTRACT

Well calibrated satellite images are not just images, but scientific data that can be used for many applications such as predicting crop growth, assessing hazard damage. Reliable radiometric calibration is crucial for expanding small satellite data use, and radiometric calibration with the Moon (called lunar calibration) is a reasonable candidate for small satellites because it does not need any special instruments other than optical sensors, and the calibration can be repeated by only conducting lunar observations in which we can treat the Moon as a well-known brightness target in space. In this study, we report a lunar calibration result for Hodoyoshi-1, which is a Japanese small satellite that has conducted lunar observations almost every month for approximately 1 year since August 2016. By comparing the observed brightness with the brightness of a simulated Moon, we successfully identified even small sensitivity variations (less than 1 %) in Hodoyoshi-1's sensors from a reference date during the observation period. Due to the advantages of lunar calibration, it is a reasonable candidate for a common radiometric calibration method for a huge number of small satellites.

INTRODUCTION

In recent years, more and more small satellites have been launched and operated for various purposes[1]. The compactness of small satellites allows frequent launch opportunities, fast development, and low costs; consequently, they have attracted great interest and are expected to expand space use.

Well calibrated satellite images are not just images, but scientific data that can be used for many applications such as evaluating the land surface environment, monitoring land use changes, predicting crop growth, assessing hazard damage. However, due to the harsh environment in space, an optical sensor inevitably experiences temporal variation of its sensitivity, which may cause incorrect brightness changes in data if we do not correct the variation. Therefore, radiometric calibration in space is essential to maintain the reliability of observed brightness, which is required to provide accurate measurement.

Considering the increasing number of small satellites, a standardized calibration method is required for comparing data obtained by different satellites that have equal radiometric accuracy. On the other hand, physical constraints on the acceptable payload and limitations of their operation and cost restrict the functionality of these small satellites. Due to these constraints and limitations, there are few satellites that have instruments for onboard calibration. A reliable and low-cost calibration method would be useful for any small satellite mission.

"Lunar calibration" is a reasonable candidate for conducting radiometric calibration for a small satellite, in which we utilize the Moon as a calibration target in space. First, because the photometric properties of the Moon have been investigated well and its brightness models have been established based on several Moon exploration missions and projects, we can consider the Moon as a well-known brightness target. Second, because the lunar calibration can be done simply by observing the Moon with the optical sensor to be calibrated, it does not require any special onboard instrument or special activity on the ground.

In addition, the Moon has long-term stable surface reflectance with a time scale of 1 million years[2]; thus we do not need to warry about temporal variation of the Moon surface in a mission period. We can conduct a Moon observation without considering any atmospheric effects, which sometimes cause large uncertainty in a calibration activity. These characteristics are also advantages of lunar calibration.

It is known that there is a somewhat large uncertainty in measuring absolute sensor sensitivity in a result from lunar calibration (approximately 10 %[3]), whereas lunar calibration is quite accurate for measuring relative sensor sensitivity variations. There have been several satellite missions in which the Moon was regularly observed and the long-term relative sensor sensitivity variations were successfully measured with an order of 0.1 % by utilizing the lunar calibration approach[4,5]. By combining the lunar calibration result with results from other calibration methods, we will obtain reliable and consistent calibration parameters.

In this study, we demonstrate the usability of lunar calibration for radiometric calibration of a small satellite through detecting temporal variations of sensor sensitivities among the Moon observations conducted by a Japanese small satellite, Hodoyoshi-1, which is operated by Axelspace Corporation. Hodoyoshi-1 observed the Moon with its visible and near-infrared multi-band sensors for the first time on August 16, 2015, and since then, it has observed the Moon almost every month for about one year.

HODOYOSHI-1 AND ITS MOON OBSERVATIONS

Hodoyoshi-1 is a Japanese small satellite that was launched on November 6, 2014 and it has successfully observed the Earth's surface with a 6.7 m ground sampling distance (GSD) for almost three years. Hodoyoshi-1 has push-broom multi-band sensors that cover blue, green, red and near-infrared bands (band B, G, R, and IR). The specifications of Hodoyoshi-1's multi-band sensors are listed in Table 1[6]. From the successful operation, Axelspace Corporation has released Hodoyoshi-1's images on their website as "image of the week[7]". Because of weight and cost limitations, the Hodoyoshi-1 is not equipped with any onboard calibration instruments.

Table 1: Specifications of Hodoyoshi-1's Push-broom sensor bands.

Wavelength [nm]	GSD [m]	Swath [km]	Bit depth [bit]
B: 450-520 G: 520-600 R: 630-690 IR: 780-890	6.7	27.8	12

The first Moon observation trial by Hodoyoshi-1 was conducted on August 16, 2016, with a phase angle of -28.9°. The phase angle is defined as the angle between the Sun, the Moon, and Hodoyoshi-1. The negative sign of the phase angle means the waxing phase of the Moon seen from Hodoyoshi-1. The second trial was conducted on August 19 with a phase angle of +9.6° (waning phase). Since November 15, 2016, Hodoyoshi-1 has observed the Moon every month (except for April 2017) with a steady phase angle (around +10°) to obtain enough bright Moon images. Only in the January observation, the Moon was taken with a negative phase angle because of operational issues. The phase angle of 10° is good for avoiding unexpected brightness fluctuation which occurs at a low phase angle condition (less than 5°)[8]. In this study, we used lunar images obtained from eight Moon observations from August 16, 2016, to May 11, 2017 (Table 2). Figure 1 shows examples of raw Moon images from the first two observations taken in Band G. It should be noted that because coefficients to convert the digital count to a value with a physical unit, such as radiance (W m^{-2} sr^{-1} μm^{-1}), have not been published yet for Hodoyoshi-1's images, we used the digital count as an indicator that is linearly related to the target brightness.

Table 2: Moon observation date and phase angles

No.	Date	Phase angle
1	2016-08-16	-28.9°
2	2016-08-19	9.6°
3	2016-11-15	10.6°
4	2016-12-14	10.7°
5	2017-01-11	-9.6°
6	2017-02-11	10.5°
7	2017-03-13	10.0°
8	2017-05-11	9.4°

The negative phase angle represents the waxing phase of the Moon, and the positive phase angle represents the waning phase.

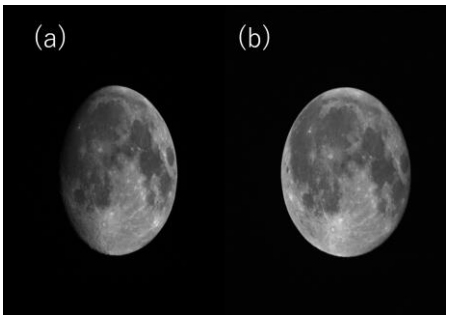

Figure 1: Examples of raw Moon images obtained in Band G (520-600 nm) on (a) August 16 and (b) August 19, 2016. Measured over sampling factors were approximately 1.3 for both (a) and (b).

Since the scan rate for a Moon observation is different from that of Hodoyoshi-1's regular operation (i.e. observing the Earth's surface), the Moon shape in an image tends to be an ellipse as shown in Figure 1. In the Hodoyoshi-1 case, the length of the Moon in the scan direction (vertical direction in the image frame) is longer than the crosstrack direction (horizontal). In this case, a region of the Moon surface oversampled by a factor based on the scan speed and the length of one-pixel field of view. This factor is called the over sampling factor[9]. To estimate the over sampling factor, we performed an ellipse fitting procedure proposed in a planetary exploration mission[10]. Using this factor, we re-sampled raw elliptical Moon images into circular Moon images, assuming the over sampling factor is constant in one observation. Figure 2 shows eight observations of the Moon conducted by Hodoyoshi-1 whose oversampling effects were corrected. Before correction of the oversampling effect, we subtracted the offset value of the image of the Moon, which was obtained from deep space where brightness should be 0, from the Moon brightness value at each pixel.

Note that we found that the over sampling factor varied from 1.3 to 1.6 in Hodoyoshi-1 observations. In addition, we found that the over sampling rate was slightly different at different lines during one observation, resulting in a distorted circular shape of the Moon after correcting the over sampling effect with a constant over sampling factor (for example, the length of the southern hemisphere is slightly shorter than that of the northern hemisphere in the scan direction).

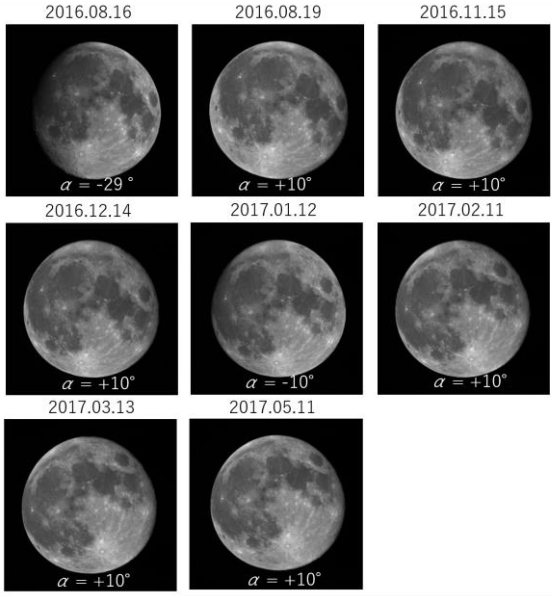

Figure 2: Moon images after correcting oversampling effect. *α* represents phase angle at observation.

LUNAR CALIBRATION WITH SIMULATED MOON OBSERVATIONS

Simulation of Moon observation with lunar reflectance model

While the surface reflectance of the Moon is stable in the long term, the Moon changes its brightness depending on the geometric conditions of solar illumination (i.e. dependency on sub-solar longitude and latitude), emission angle to the observer (i.e. dependency on sub-observer longitude and latitude), and phase angle of the Sun, the Moon, and the observer due to the complicated surface features of the Moon and the photometric characteristics of the Moon surface[8]. To use the Moon as a calibration target, such geometric dependence of observed Moon brightness should be canceled for extracting only the temporal variation of sensor sensitivity. For this, a reliable lunar brightness model is required that can simulate the geometric dependence.

Recently, a hyperspectral lunar surface brightness model based on hyperspectral observation data obtained by Spectral Profiler (SP)[11] onboard SELENE, a Japanese lunar orbiter, has been proposed and its reliability has been investigated[11]. This SP model covers a wavelength range from 516 nm to 1600 nm with a 6-8 nm spectral sampling interval, which allows to treat various sensors with different spectral response functions. The SP model also contains the reflectance of the whole lunar surface with a 0.5° interval in the Moon latitude and longitude[8], which enables the simulation of Moon observations in any geometric conditions.

For a simulation of a Moon observation, the required parameters are the distance between the Sun and the Moon, distance between the Moon and the observer, sub-solar latitude and longitude, and sub-observer latitude and longitude on the Moon. These parameters were obtained from Hodoyoshi-1 trajectory information measured from the two-line elements (TLEs) distributed by the North American Aerospace Defense Command (NORAD), and trajectory information of the Sun, the Earth, and the Moon was measured from SPICE toolkits distributed by NASA[13]. Figure 3 shows a simulated Moon image with an observation geometry on August 19, 2016. In the lunar calibration method based on the SP model, even a distorted Moon shape can be simulated by distorting the simulated Moon image based on a cross-correlation approach and affine transformation[11]. Note that, in this study we only considered Moon images obtained with Band G and R because the wavelength range of Band B (450-520 nm) is mostly outside of the SP model, and we found the observations with Band IR were unstable, resulting in the Moon positions being out of the field of view in some images.

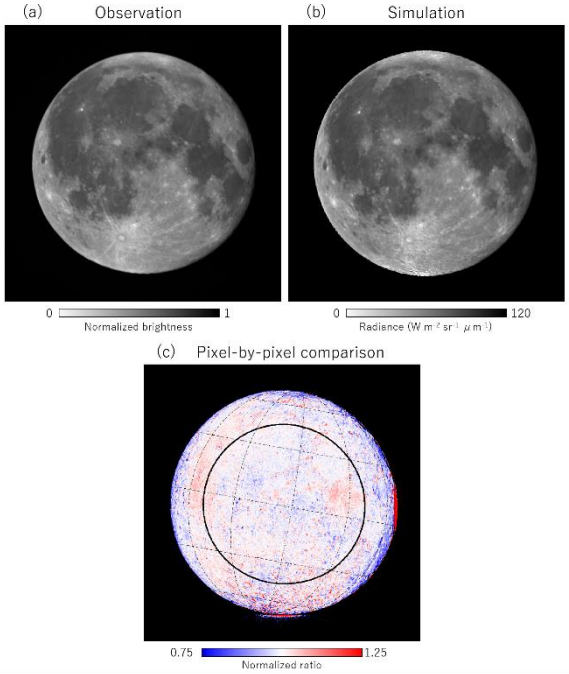

Figure 3: Comparison of (a) observed (August 19, 2016) and (b) simulated Moon images (Band G), and (c) their brightness ratio normalized by the mean value. A region surrounded by a black circle in (c) represents a reliable region for the comparison (incident angle < 60° and emission angle < 45°).

Figure 4 shows a frequency plot from pixel-by-pixel brightness comparison between the observed and simulated Moon images based on Figure 3c. In this comparison, we limited the Moon pixels to those whose solar incident angles are less than 60° and emission angles are less than 45°, following Kouyama et al (2016)[11]. By fitting a simple linear function whose offset is zero (i.e. $y = ax$) to the frequency plot shown in Fig. 4, we confirmed that the uncertainty of the slope value is less than 0.02 %, which was measured from the standard deviation of residuals between the fitting function and the brightness distribution. This indicates Band G has a good linearity at least within the brightness range of the Moon. The small uncertainty is also confirmed in Band R. In addition, the correlation coefficient between the observed and simulated Moon images was more than 0.98. This high correlation coefficient indicates that the simulated image based on the SP model is statistically similar to the observation, so it can be used for the lunar calibration.

Measuring sensor sensitivity degradation

Since we can assume that there is no sensor sensitivity degradation in a simulation of a Moon image, we can understand how much sensor sensitivity degrades at an observation through a comparison of the observed and simulated brightness of the Moon. In this study, we investigated the time variation of the relative sensor sensitivity of a sensor by normalizing the brightness ratio of observation over simulation at a reference date as:

$$s(t) = \frac{r(t)}{r(t_0)} \qquad (1)$$

where s is the relative sensor sensitivity at an observation date (t) compared to the sensitivity at a reference date (t_0), and r is the brightness ratio (observed / simulated). We used an observation on August 19, 2016 for the reference.

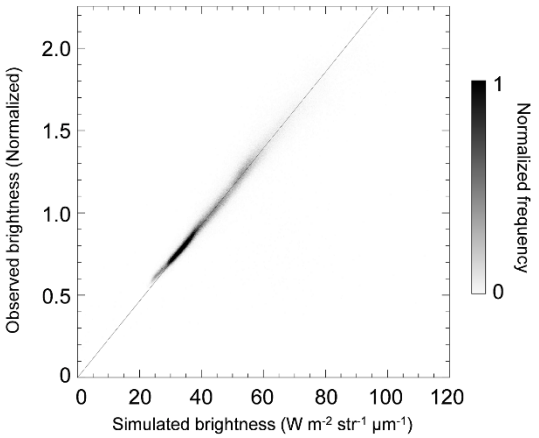

Figure 4: Frequency plot of observed digital counts and simulated brightness of Moon shown in Figure 3. Observed values are normalized by their mean value. Linear fitting result is shown with a gray line.

This approach is suitable for a lunar calibration approach with SP model that has a large uncertainty in the absolute value of the reflectance (several tens of %[11, 15]), because the uncertainty in the absolute value can be canceled out in measuring the relative value.

Figure 5 shows the temporal variations of the sensor sensitivities of Band G and R. In both bands, the sensitivity degradations can be identified, even though their magnitudes were smaller than 1 % during the Moon observation period. Based on a calibration study of an Earth observation sensor[14], the magnitude of relative radiometric degradation, D, can be represented by the following form:

$$D(t) = (1 - C_2)\exp\{-C_1(t - t_0)\} + C_2, \qquad (2)$$

where C_1 and C_2 are the parameters to be fitted, and t_0 is August 19, 2016, which corresponds to 651.8 days since Hodoyoshi-1 was launched. By fitting $D(t)$ to the measured sensitivities in Figure 5, we estimated that C_1

and C_2 are 0.00974 and 0.993 for Band G and 0.000645 and 0.963 for Band R, respectively.

From the fitting result, Band G showed a relatively rapid degradation trend at first, and then the degradation speed decreased. On the other hand, Band R shows a more continuous degradation trend during the Moon observation period than that in Band G. Although the phase angles were different on August 16, 2016 (phase angle: -28.8°) and January 11, 2017 (-9.6°) from the phase angles at other observations (approximately 10°), their deviations (up to 0.2%) were comparable to the others, indicating the reliability of the phase angle dependence of SP model. Since the standard errors between the fitted model and sensor sensitivities of Band G and R were almost 0.1%, the magnitude of the possible uncertainty in this lunar calibration result could be of the order of 0.1%. More observations will provide a more concrete conclusion in future.

CONCLUSION

Hodoyoshi-1 has conducted Moon observations for radiometric calibration of its sensors since August 2016. The target phase angle was around 10° to have a stable lunar brightness among observations. The sensor sensitivity variations of Band G and R were investigated with eight Moon observations by comparing the observed brightness and simulated Moon brightness based on the SP model. In both Band G and R, sensor sensitivity degradations whose magnitudes were even less than 1 % were successfully identified. In other words, by utilizing a lunar calibration method, we may detect a sensor sensitivity variation with an accuracy of more than 1 %. Since Hodoyoshi-1 will continue lunar observations, more detailed sensor sensitivity variation will be investigated.

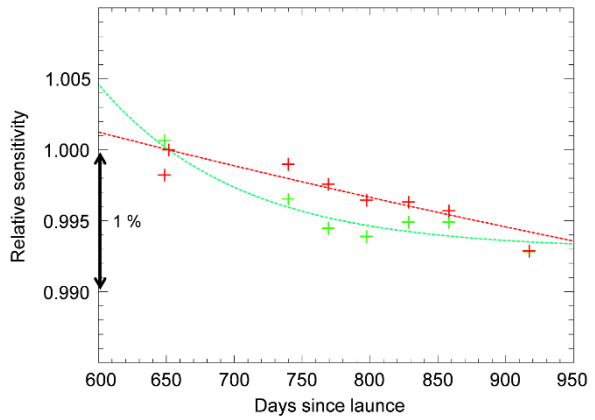

Figure 5: Temporal variations of sensor sensitivities of Band G and R normalized by those on August 19, 2016. Green and red crosses are results from Band G and R, respectively. Dashed curves are fitted degradation curves.

Lunar calibration can be applied without any special instruments other than optical sensors if thermal balance and attitude control of the satellite allows it to observe the Moon. Therefore, the lunar calibration can be a candidate for a common radiometric calibration method for a huge number of small satellites, which usually have strict weight and cost restrictions.

Acknowledgments

The authors thank Axelspace Corporation for providing Hodoyoshi-1 Moon observation images and useful information to evaluate Moon brightness. This study is partly supported by the New Energy and Industrial Technology Development Organization (NEDO).

References

1. E. Buchen, "Small satellite market observations," in *Proc. 29th Annual AIAA/USU Conference of Small Satellite*. Logan, UT, USA, pp. 8–13, 2015.
2. H. H. Kieffer, "Photometric Stability of the Lunar Surface," *Icarus*, 130, pp. 323–327, 1997.
3. T. C. Stone, "Radiometric Calibration Stability and Inter-calibration of Solar-band Instruments in Orbit Using the Moon", Orbit," *in Proc. SPIE—Earth Observing Systems XIII*, 2008.
4. R. E. Eplee, R. A. Barnes, F. S. Patt, G. Meister, and C. R. McClain, "SeaWiFS Lunar Calibration Methodology after Six Years on Orbit," in *Proc. SPIE—Earth Observing Systems IX*, 5542, pp. 1-13, 2004.
5. X. Xiong, K. Butler, K. Chiang, B. Efremova, J. Fulbright, N. Lei, J. McIntire, H. Oudrari, Z. Wang, and A. Wu, "Assessment of S-NPP VIIRS On-Orbit Radiometric Calibration and Performance," *Remote Sens.*, 8, 84, 2016.
6. https://www.axelspace.com/en/solution_/hodoyoshi1/
7. https://www.axelglobe.com/en/
8. Y. Yokota, T. Matsunaga, M. Ohtake, J. Haruyama, R. Nakamura, S. Yamamoto, Y. Ogawa, T. Morota, C. Honda, K. Saiki, K. Nagasawa, K. Kitazato, S. Sasaki, A. Iwasaki, H. Demura, N. Hirata, T. Hiroi, R. Honda, Y. Iijima, and H. Mizutani, "Lunar photometric properties at wavelengths 0.5-1.6 μm acquired by SELENE Spectral Profiler and their dependency on local albedo and latitudinal zones," *Icarus*, 215, pp. 639–660, 2011.

9. H. H. Kieffer and T. C. Stone, “The spectral irradiance of the Moon,” *Astron. J.*, 129, pp. 2887–2901, 2005.

10. K. Ogohara, T. Kouyama, H. Yamamoto, N. Sato, M. Takagi, and T. Imamura, “Automated cloud tracking system for the Akatsuki Venus Climate Orbiter data,” *Icarus*, 217, pp. 661–668, 2012.

11. T. Matsunaga, M. Ohtake, Y. Hirahara, and J. Haruyama, “Development of a visible and near infrared spectrometer for Selenological and Engineering Explorer (SELENE),” in *Proc. SPIE Int. Soc. Opt. Eng.*, 4151, pp. 32–39, 2001.

12. T. Kouyama, Y. Yokota, Y. Ishihara, R. Nakamura, S. Yamamoto, T. Matsunaga, “Development of an application scheme for the SELENE/SP lunar reflectance model for radiometric calibration of hyperspectral and multispectral sensors,” *Planet. Space Sci.*, 124, pp. 76–83, 2016.

13. C. H. Acton, “Ancillary Data services of NASA's navigation and ancillary information facility,” *Planet. Space Sci.*, 44, pp. 65–70, 1996.

14. S. Tsuchida, H. Yamamoto, and A. Kamei, “Long-term vicarious calibration of ASTER VNIR bands,” In *Proc of the 52nd Conference of the Remote Sensing Society of Japan*, pp. 85–86, 2012.

15. M. Ohtake, C. M. Pieters, P. Isaacson, S. Besse, Y. Yokota, T. Matsunaga, J. Boardman, S. Yamomoto, J. Haruyama, M. Staid, U. Mall, and R. O. Green, “One Moon, Many Measurements 3: Spectral reflectance,” *Icarus*, 226, pp. 364–374, 2013.